scientific reports

Check for updates

OPEN

CSF carnitine is a potential biomarker in paediatric tuberculous meningitis

Ontefetse Neo Plaatjie[1], A. Marceline Tutu van Furth[1,2], Regan Solomons[3], Martijn van der Kuip[2,4] & Shayne Mason[1,4]✉

The poor outcome of tuberculous meningitis (TBM) is largely due to the difficulty of diagnosis caused by nonspecific symptoms and the absence of specific and sensitive tests. Carnitines regulate energy metabolism, and their elevation has been consistently reported in the cerebrospinal fluid (CSF) of TBM patients. We employed a targeted liquid chromatography-tandem mass spectrometry (LC-MS/MS) approach to investigate the acylcarnitine metabolome in paediatric TBM, comparing it to non-meningitis controls (NMC) and viral meningitis (VM). We also investigated correlations of significant acylcarnitines with clinical metadata. We found that short-chain acylcarnitines were significantly elevated in TBM. Acetylcarnitine, propionylcarnitine, and butyrylcarnitine demonstrated significant diagnostic potential in distinguishing between TBM and control groups, with 80–90% specificity and 70–80% sensitivity. Free carnitine stood out as the strongest potential marker for TBM, distinguishing TBM from NMC (100% specificity, 90% sensitivity) and VM (80% specificity, 90% sensitivity). Furthermore, free carnitine is strongly correlated with basal meningeal enhancement and hydrocephalus, key neuroradiological markers of TBM. Free carnitine could serve as a potential biomarker for TBM, as well as a marker of TBM severity. Our results suggest that disruptions in fatty acid and energy metabolism in TBM cases are important because free carnitine plays a crucial role in the β-oxidation of fatty acids by transporting long-chain fatty acids into the mitochondria for energy production.

Keywords Acylcarnitines, Paediatric, Tuberculous meningitis, Cerebrospinal fluid (CSF), Liquid chromatography tandem mass spectrometry (LC-MS/MS)

Tuberculous meningitis (TBM) is the most severe form of extrapulmonary tuberculosis (TB). *Mycobacterium tuberculosis* (*M.tb*) can disseminate from the lung via hematogenous spread, affecting multiple sites, including the central nervous system (CNS). After crossing the blood-brain barrier (BBB), local leptomeningeal inflammation and subsequent granuloma formation in the subpial brain parenchyma result in TBM[1]. Within the paediatric population, infants and young children are particularly susceptible due to an underdeveloped immune system[2]. The incidence of TB in children is increasing steadily, highlighting an urgent public health concern. According to the World Health Organisation (WHO), children under 15 years accounted for 11% of the estimated global TB cases in 2019[3], with an estimated 24,000 children who developed TBM that year[4]. By 2023, the proportion of TB cases in children aged 0–14 years had risen to 12%[5]. This trend highlights the urgent need for prompt and effective interventions to address paediatric TBM.

Diagnosing TBM is challenging, primarily due to its nonspecific clinical symptoms, which often result in late recognition, coupled with the lack of sensitive diagnostic tools for disease detection[6]. Diagnosis relies on a combination of clinical history, physical examination (symptoms and signs), cerebrospinal fluid (CSF) analyses (increased white cell count, elevated protein, and low glucose levels), microbiological confirmation by culture and/or molecular technique, and neuroimaging showing basal meningeal enhancement, infarction, hydrocephalus, or tuberculomas[7,8]. Early diagnosis has been shown to improve clinical outcomes in children[9],

[1]Department of Biochemistry, Human Metabolomics, Faculty of Natural and Agricultural Sciences, North-West University, Potchefstroom, South Africa. [2]Department of Paediatric Infectious Diseases and Immunology, Amsterdam University Medical Center, Emma Children's Hospital, Amsterdam, The Netherlands. [3]Department of Paediatrics and Child Health, Faculty of Medicine and Health Sciences, Stellenbosch University, Cape Town, South Africa. [4]Martijn van der Kuip and Shayne Mason have contributed equally as last authors ✉email: nmr.nwu@gmail.com

while delayed diagnosis is associated with high mortality rates or long-term neurological deficits, despite treatment[10,11].

Despite advancements in diagnostic technologies, TBM remains difficult to diagnose. The standard uniform TBM case definition by Marais et al.. (2010)[8] incorporates diagnostic methods such as CSF culture, which can take up to six weeks to produce results[12]. The WHO recommends the next-generation Xpert MTB/RIF Ultra (Xpert Ultra) for initial diagnostic testing for children and adults suspected of TBM. Xpert Ultra offers a sensitivity of 44–77% in adults and improves detection; however, the assay lacks sufficient predictive value to reliably exclude TBM when the result is negative[13–15]. This limitation is even more pronounced in children, where bacteriological confirmation of TBM is often lacking, making Xpert Ultra an inadequate sole diagnostic tool for paediatric TBM cases[6,7]. Hence, there is a pressing need to develop rapid, highly sensitive, and specific diagnostic tests for TBM to ensure timely and accurate diagnosis, especially in vulnerable populations such as children. Omics approaches, including proteomics and metabolomics, are increasingly used to identify specific disease markers and gain deeper insights into pathophysiological mechanisms. For example, studies analysing CSF in childhood TBM have identified disease-specific biomarker patterns, which may aid in diagnosis and understanding disease pathogenesis[16,17].

Metabolomics, a rapidly growing field of omics, provides a powerful tool for identifying and analysing altered metabolites that could potentially contribute to improving TBM diagnosis[18]. The CSF complements this approach by serving as a valuable medium for studying biochemical changes in the brain, as it directly reflects alterations in the CNS. Advancements in CSF metabolomics studies have profiled the CSF metabolome of TBM cases, establishing a foundation for altered metabolites and their related pathways that warrant further investigation[19]. Energy metabolism, particularly the carbohydrate and glucose metabolism, which serve as the primary energy source for the CNS, is among the notable perturbed pathways reported in TBM[20–24].

Tomalka et al.[22] reported elevation of multiple CSF carnitines and lactate in patients with TBM and attributed this alteration to simultaneous activation of β-oxidation of fatty acids and glycolysis – a process indicative of enhanced energy production. Similarly, Van Zyl et al.[23] reported elevated levels of L-carnitine in children with TBM. Carnitines play a critical role in regulating energy metabolism, particularly by facilitating the transport of long-chain fatty acids into the mitochondria for energy production during periods of high-energy demand[25,26]. The observed trend in TBM indicates increased energy demand, prompting the body to seek alternative energy sources beyond glucose, including the use of fatty acids for energy production. This is reflected in the consistent alteration of carnitines in TBM. Furthermore, a study by Dai et al.. (2017)[27] reported increased synthesis and degradation of ketone bodies, along with elevated levels of unsaturated fatty acids in TBM. These findings provide further evidence of elevated energy demands in TBM, as the body tends to preferentially use ketone bodies for energy production over fatty acids during prolonged energy stress.

There is evidence of altered carnitines in other various types of neuroinfectious diseases[22,23,26,28,29]. However, despite this compelling evidence, none of these studies have specifically focused on the acylcarnitine (conjugate of carnitine and fatty acids) pathways, especially in children with TBM, to evaluate the extent of their alterations and their potential as diagnostic biomarkers. This highlights a critical gap that this study aims to address. In this study, we aim to comprehensively profile and compare the acylcarnitine metabolome in CSF samples from paediatric TBM, viral meningitis (VM), and non-meningitis control (NMC) groups using a targeted liquid chromatography tandem mass spectrometry (LC-MS/MS) approach. By characterising these metabolic changes, we endeavour to uncover their potential role in the immunopathogenesis of TBM and assess their potential to differentiate TBM from VM. We also explore the correlations of acylcarnitines with clinical data, CSF features, and neuroimaging, magnetic resonance imaging (MRI), and computed tomography (CT), and findings of the brain to enhance our understanding of disease mechanisms.

Materials and methods

Patient selection and ethics

This study retrospectively collected CSF from a historical cohort of paediatric patients between 2009 and 2013. The paediatric (≤ 12 years old) sample group used in this study resides in an area endemic for TB – the Western Cape Province of South Africa[30]. Each participant was referred from a local regional clinic to the paediatric service at Tygerberg Hospital, a tertiary hospital in the Eastern Metropole of Cape Town, for meningitis screening. After assessment by the paediatric neurology team, CSF samples were collected via lumbar puncture for differential diagnostic purposes. Written, informed consent and/or assent were obtained for CSF samples for research purposes. This study was approved by the Health Research Ethics Committee (HREC) of Stellenbosch University, Tygerberg Hospital (ethics approval no. N16/11/142), the Western Cape Provincial Government, and the HREC of the North-West University, Potchefstroom campus (ethics approval no. NWU-00,063-18-A1-05).

Sample collection, handling, and storage

This study included a total of 144 participants: NMC ($n = 57$), VM ($n = 31$), and TBM ($n = 56$). The control group included patients initially suspected of having meningitis based upon clinical symptoms but later confirmed negative for meningitis. VM and TBM cases were subdivided into 'probable' and 'definitive' classifications. For VM, a 'definite' VM ($n = 13$) diagnosis was assigned based on a positive viral PCR test, whereas a 'probable' VM ($n = 18$) diagnosis was given if the PCR test was negative, but the patient presented with clinical symptoms of VM and CSF pleocytosis (> 5 leucocytes/mm^3). For TBM, a 'definite' ($n = 23$) and 'probable' ($n = 33$) TBM diagnosis was assigned based on a uniform case definition given by Marais et al. (2010)[8]. The demographic and clinical characteristics of all patients are presented in Table 1. The main exclusion criterion for all participants was HIV-positive/unknown cases. Following lumbar puncture, all CSF samples were stored at -80℃ and transported on ice to the biosafety level 3 (BSL3) lab at Human Metabolomics at North-West University, Potchefstroom campus, South Africa. Upon arrival, the samples were subjected to a cleaning (filtration) procedure as a safety precaution

		Tuberculous meningitis (*n* = 56)	Non-meningitis controls (*n* = 57)	Viral meningitis (*n* = 31)
Clinical symptoms [*n*(%)]				
Age in months [median (range)]		47 (8–144)	45 (5–168)	68 (5–156)
Sex	Female	29 (52)	20 (35)	8 (26)
	Male	27 (48)	37 (65)	23 (74)
Tuberculous meningitis stage	Stage I	8 (15)	N/A	N/A
	Stage II	20 (37)		
	Stage III	26 (48)		
Fever		45 (82)	34 (60)	28 (90)
Vomiting		39 (70)	27 (47)	23 (74)
Diarrhea		7 (13)	12 (21)	5 (16)
Weight loss		24 (43)	8 (14)	0
Headache		21 (38)	17 (30)	23 (74)
Raised ICP		7 (13)	1 (2)	1 (3)
Meningeal irritation		16 (29)	8 (14)	14 (45)
Seizure		15 (27)	21 (37)	2 (6)
Cough		20 (36)	16 (28)	7 (23)
Decreased consciousness		11 (20)	11 (19)	4 (13)
Neuroimaging parameters [n(%)]				
Hydrocephalus		44 (79)	1 (2)	0
Basal enhancement		41 (73)	3 (5)	1 (3)
Infarctions		14 (25)	1 (2)	1 (3)
Brainstem dysfunction		7 (13)	1 (2)	1 (3)
Tuberculomas		11 (20)	0	0
Cerebrospinal fluid features [median (range)]	Normal values [33, 34]			
Glucose (mM)	2.77–4.44	2 (1.2–3.2)	3.8 (3.40–4.30)	3.5 (3.15–3.90)
Protein (g)	0.15–0.6	1.13 (0.81–3.2)	0.2 (0.15–0.27)	0.39 (0.23–0.59)
Erythrocytes (cells/μL)	–	4 (0.0–74.50)	0 (0.0–1.0)	2 (0–30.5)
Leucocytes (cells/μL)	0–5	58 (22.5–173.5)	0 (0.0–1.5)	78 (35–197.50)
PMNs (cells/μL)	0–5	3(0.0–12.0)	0 (0–0)	20 (0–28.50)
Lymphocytes (cells/μL)	< 5	55 (17.0–126.0)	0 (0.0–1.0)	49 (19–121)

Table 1. Patient baseline characteristics. Data are presented as n (%) for categorical variables and median (range) for continuous variables. ICP = intracranial pressure; PMNs = polymorphonuclear neutrophils.

to enable the safe general use of the samples. All samples were filtered in the BLS3 lab using Amicon Ultra-2 mL 10,000 MWCO centrifugal filters at 4,500 x *g* for 20 min. Each supernatant was recollected in a clean sample collection tube, which was sterilised by wiping the tubes externally with 70% ethanol and re-labelled as per the original sample tube. All filtered samples were stored immediately at − 80 °C until further use.

Reagents and chemicals

UPLC-grade solvents (water and acetonitrile) were sourced from Anatech (Burdick and Jackson). Formic acid and sodium chloride were purchased from Merck (South Africa), while acetyl chloride and 1-butanol were obtained from Sigma-Aldrich (South Africa). A total of 11 acylcarnitine reference standards were purchased from Cerilliant (Sigma-Aldrich): short-chained acylcarnitines (L-carnitine, acetylcarnitine, propionylcarnitine, butyrylcarnitine and isovalerylcarnitine), medium-chained acylcarnitines (hexanoylcarnitine and octanoylcarnitine), and long-chained acylcarnitines (decanoylcarnitine, dodecanoylcarnitine, tetradecanoylcarnitine and octadecanoylcarnitine) (Table S2). Deuterated free carnitine (methyl-d3-L-carnitine) and acylcarnitines (d3-acetylcarnitine; d3-propionylcarnitine; d3-butyrylcarnitine; d9-isovalerylcarnitine; d3-octanoylcarnitine; d3-decanoylcarnitine; d3-dodecanoylcarnitine; d3-tetradecanoylcarnitine; d3-octadecanoylcarnitine) served as internal standards.

Sample matrix optimisation

Before sample preparation and analysis, the analytical method was optimised for the CSF sample matrix. Briefly, pooled CSF was obtained from Tygerberg Hospital and subjected to a filtration cleaning procedure, as detailed in the sample handling section. Following filtration, the pooled CSF was stripped of metabolites through a dialysis procedure. A saline solution was prepared by dissolving 9 g of sodium chloride in 1 L of deionised water. The filtered pooled CSF (7 mL) was transferred into a dialysis membrane (1–10 kDa), which was submerged in the saline solution and placed on a shaker for 48 h. The saline solution was freshly prepared and replaced every 24 h to ensure the effective removal of metabolites. The stripped CSF volume was used to spike known concentrations

of acylcarnitine standards to create calibrators and served also as a sample matrix blank. The stripped and spiked CSF was stored at − 80 °C until further analysis.

Sample preparation

Prior to analysis, all CSF samples were thawed to room temperature and homogenised by vortex mixing. For extraction, 10 µL of each CSF sample was spiked with 200 µL of an internal standard working solution prepared in methanol. The same procedure was applied to calibrators and pooled quality control (QC) samples. The mixtures were vortexed for 30 s and centrifuged at 12,000×g at 10 °C for 10 min. The internal standard solution contained deuterated acylcarnitines. Pooled QC samples were prepared by combining small aliquots from individual samples into a single tube, which was aliquoted into vials, stored at – 80 °C and analysed with each batch. The sample supernatant (200 µL) was carefully transferred to clean Eppendorf tubes and evaporated to dryness under a gentle stream of nitrogen gas for approximately 1 h. To derivatise the samples, 100 µL of N-butanol: acetyl chloride (25:6.25, v/v) was added to the dried residue, and the samples were incubated for 45 min at 65 °C. Thereafter, the butylated samples were evaporated at 37 °C to dryness under a gentle stream of nitrogen gas. The dried residue was reconstituted with 100 µL of a freshly prepared mobile phase (acetonitrile: water (50:50) (v/v), with 0.1% formic acid). The samples were thoroughly vortex-mixed to dissolve the dried compounds. The samples were transferred to LC vials and loaded onto an Agilent LC-QQQ 6470 autosampler for analysis.

LC-MS/MS analysis

The LC-MS/MS analysis was carried out as described by Terburgh et al. [31], with slight modifications. Briefly, the analysis was carried out using a high-performance liquid chromatography 1200 infinity system (Agilent Technologies, USA) coupled to a triple quadrupole mass spectrometer 6470 QQQ. The separation of acylcarnitines was achieved by a chromatographic separation using a C18 Zorbax reverse phase column (2.1 mm × 100 mm × 1.8 µm, Agilent Technologies, USA) fitted with a Phenomenex guard column (2.0 µm depth filter × 0.004in ID). The column temperature was kept at 30 °C. during the entire run. The mobile phase consisted of water with 0.1% formic acid (A) and acetonitrile with 0.1% formic acid (B). The gradient elution started with 5% B at 0 min, followed by a linear gradient to 100% B at 13 min. The gradient was kept at 100% B for five min and then decreased to 5% within two min, followed by re-equilibration for eight min to maintain reproducibility. The flow rate was 0.3 mL/min for the first 13 min, after which it was increased to 0.35 mL/min for the rest of the run. The total run time for each sample was approximately 30 min. The samples were delivered to the QQQ-MS via electrospray ionisation (ESI) in positive mode with the source conditions set as follows: nitrogen drying gas temperature of 300 °C and flow of 7.5 L/min, a nebuliser pressure of 30 psi, and capillary voltage of 3500 V. The compounds were analysed in multiple reaction monitoring (MRM) mode using enhanced sensitivity with the multiplier voltage set at 300 Delta EMV and a dwell time of 45 milliseconds for all metabolites. The parameters for each butylated compound and isotopically labelled standard are given in Table S1. Agilent's MassHunter Workstation Software (v B02.01; data acquisition for 6400 Series Triple Quadrupole) and MassHunter Optimizer software (v B02.01) were used for data acquisition in the MRM configuration settings.

Data processing and quality control

Data was extracted using Agilent's MassHunter Workstation software (v B06.00; Qualitative Analysis and Quantitative Analysis. Samples and metabolites were individually inspected, aligned with their respective internal standards, and integrated manually. The extracted metabolite responses were then exported to an Excel file for subsequent quantification and data filtering. Relative concentrations of the analytes were determined based on the peak area ratios to the corresponding internal standards. The relative standard deviation (RSD) was calculated using QC samples, and metabolites with an RSD greater than 30% were excluded from further analysis. Principal component analysis (PCA) was performed to evaluate the clustering of the QC data, as illustrated in Fig. S1.

Statistical analysis

Statistical analyses were performed using MetaboAnalyst version 6.0 (www.metaboanalyst.ca/). Principal component analysis and k-means clustering were first performed to explore the data trend. Analysis of variance (ANOVA) was performed to assess significant differences in acylcarnitine levels across the three experimental groups. A p-value of less than 0.05 was considered statistically significant. For metabolites showing significant differences, the effect size was calculated (in Excel) using Cohen's d-value, with a value greater than 0.8 indicating a large effect. Metabolites that were not significantly different between groups were excluded from further statistical analysis. A receiver operating characteristic (ROC) analysis was conducted to investigate the diagnostic potential of significant metabolites. Correlation analysis between acylcarnitines levels and clinical data, CSF cell count, and neuroimaging findings was calculated using Spearman-rank correlation.

Results

Baseline clinical characteristics

Fifty-six children with TBM were included in this study. Their median age was 47 months, and 29 (52%) were female. Most patients presented with severe disease (48% stage III), followed by moderately severe (37% stage II) and early-stage (15% Stage I) disease according to the refined MRC grading system[32]. Clinical characteristics, CSF features, and neuroimaging parameters are presented in Table 1.

Acylcarnitine analysis

First, an exploratory analysis was done using an unsupervised PCA score plot to evaluate group differences among the following comparisons: NMC vs. TBM and VM, probable vs. definite TBM, and the three stages of TBM. We observed a notable separation between TBM and VM, as well as between the NMC and TBM groups; however, no clear separation was observed between the NMC and VM groups (Fig. 1A). Similarly, PCA showed no clear separation between probable vs. definite TBM and the different stages of TBM (Fig. S6). We further performed k-means clustering to explore how the groups clustered together. This analysis revealed that NMC and VM samples predominantly clustered together in cluster 1, while the majority of TBM samples clustered in cluster 2 (Fig. 1B). Our exploratory and cluster analysis suggests that the NMC and VM groups may share similar acylcarnitine profiles, while TBM exhibits distinct acylcarnitine metabolic characteristics.

Significantly altered acylcarnitines

ANOVA was used to assess the significant differences of acylcarnitines across the three groups. Out of eight acylcarnitines, only five [L-carnitine (C0), acetylcarnitine (C2), propionylcarnitine (C3), butyrylcarnitine (C4), and isovalerylcarnitine (iC5)] were found to be statistically significant (p-value < 0.05), the majority of which were short-chain acylcarnitines (Figs. 2A–E). Notably, of all the significant acylcarnitines, only L-carnitine (C0) and isovalerylcarnitine (iC5) significantly differentiated TBM from NMC and TBM from VM, but did not differentiate VM from NMC. Medium- and long-chain acylcarnitines did not show significant differences across the groups (p-value > 0.05) (Figs. S7A–C).

Effect size

The effect sizes of the five significant metabolites were determined using Cohen's d-value to measure how much the metabolites contributed to the differences between the groups (i.e., practical significance). A Cohen's d-value greater than 0.8, indicating a large effect, was used as a threshold. The three metabolites (acetylcarnitine, propionylcarnitine, and butyrylcarnitine) that statistically differentiated the NMC group from the VM group showed a smaller effect size (Cohen's d-value < 0.8, Fig. 3). For TBM vs. VM and NMC vs. TBM, four metabolites (L-carnitine; acetylcarnitine; propionylcarnitine; butyrylcarnitine) exhibited large effect sizes (Cohen's d-value > 0.8, Fig. 3), with L-carnitine demonstrating the most substantial differentiation between TBM and the other two groups. Conversely, isovalerylcarnitine, despite having a p-value less than 0.05, showed a smaller effect size in distinguishing TBM from the other groups. Four metabolites (L-carnitine; acetylcarnitine; propionylcarnitine; butyrylcarnitine) demonstrated a larger effect size (Cohen's d > 0.8) and a p-value less than 0.05 and were included for subsequent statistical analysis.

Evaluation of diagnostic markers for TBM

A receiver operating characteristic (ROC) analysis was performed to evaluate the diagnostic performance of the four significantly altered metabolites for differentiating between the groups. Excellent classification was assigned to metabolites with an area under the curve (AUC) greater than 0.8, according to Hosmer and Lemeshow (2000)[35]. Between the NMC and TBM groups, L-carnitine showed excellent diagnostic accuracy,

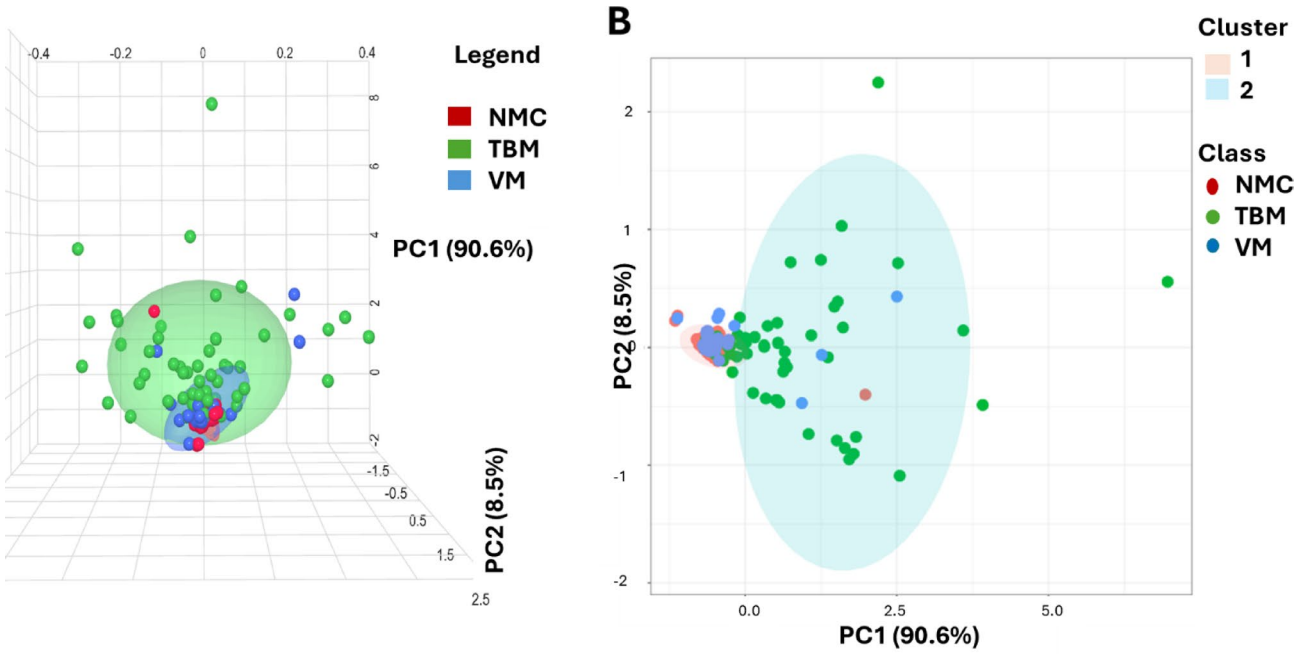

Fig. 1. (**A**) PCA score plots and (**B**) k-means clustering of control (NMC) vs. TBM and VM. The control and VM groups share similar acylcarnitine metabolic profiles, while TBM cases show a distinct acylcarnitine metabolic profile.

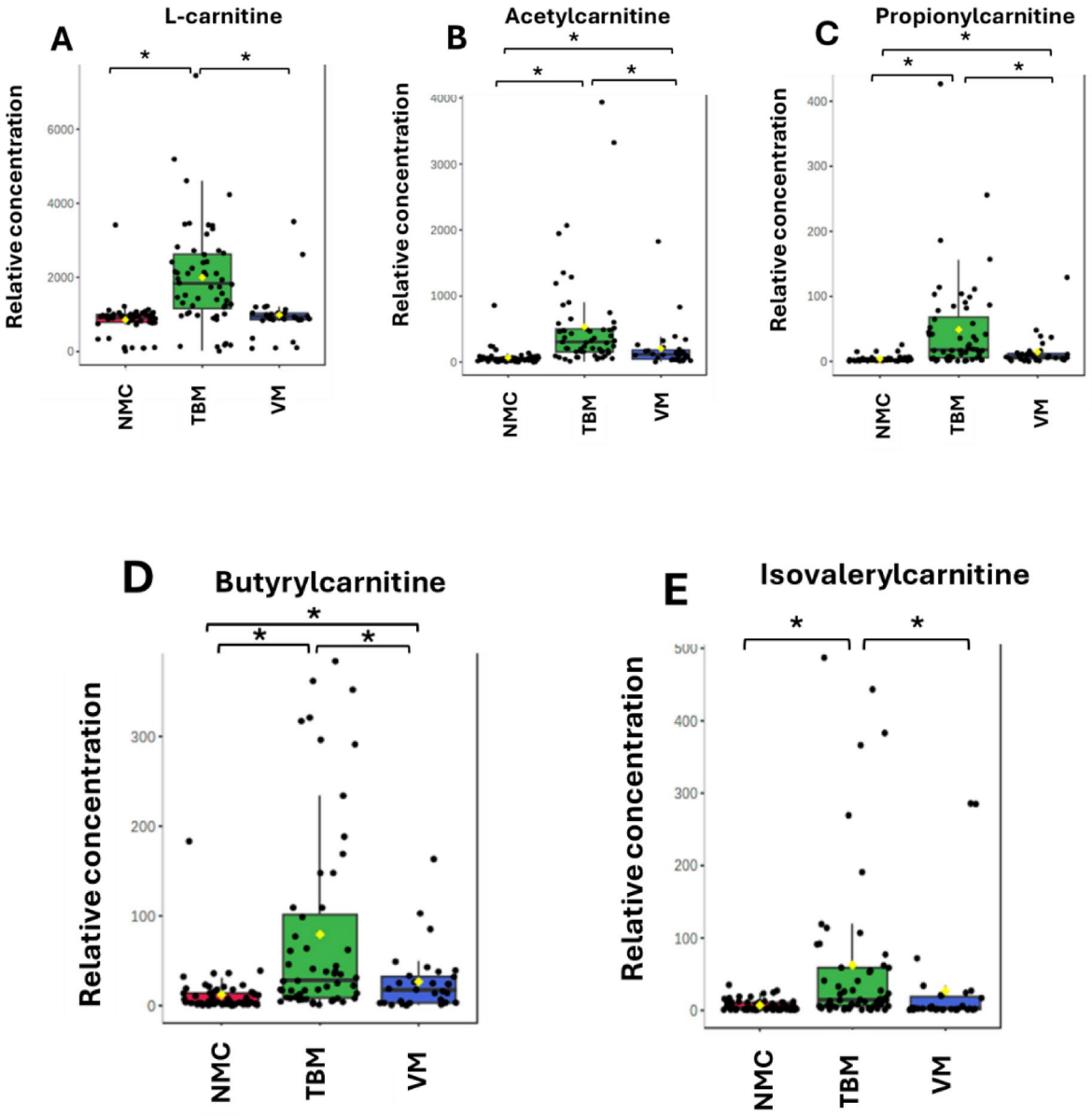

Fig. 2. Box plots of the significant acylcarnitines that differentiated the groups – control (NMC, red); TBM (green); VM (blue). Metabolite concentrations are expressed as relative concentrations. A p-value < 0.05 is indicated by *.

with an AUC of 0.928 (95% CI, 0.872–0.975), indicating high discrimination. L-carnitine also demonstrated good diagnostic accuracy between TBM and VM, with an AUC of 0.864 (95% CI, 0.764–0.951). In contrast, L-carnitine demonstrated poor diagnostic performance between the NMC and VM comparison, with an AUC of 0.587 (95% CI, 0.463–0.703), indicating poor discrimination (Figs. 4A–C). For acetylcarnitine, excellent diagnostic accuracy was observed between the NMC and TBM, compared with an AUC of 0.919 (95% CI, 0.859–0.959). In a comparison between TBM vs. VM and NMC vs. VM, acetylcarnitine demonstrated moderate diagnostic accuracy with AUCs of 0.747 (95% CI, 0.637–0.855) and 0.761 (95% CI, 0.632–0.87), respectively. Propionylcarnitine revealed a great diagnostic accuracy between the NMC and TBM groups with an AUC of 0.89 (95% CI, 0.809–0.946). Between TBM vs. VM and NMC vs. VM, propionylcarnitine showed a moderate diagnostic accuracy with AUC of 0.747 (95% CI, 0.638–0.841) and 0.79 (95% CI, 0.679–0.885), respectively. Butyrylcarnitine showed a good diagnostic accuracy between TBM and NMC with an AUC of 0.807 (95% CI, 0.73–0.878) and demonstrated a fair diagnostic accuracy between TBM vs. VM and NMC vs. VM with AUCs of 0.641 (95% CI, 0.534–0.753) and 0.706 (95% CI, 0.588–0.822), respectively. Overall, L-carnitine was the most promising diagnostic biomarker specific to TBM. We further performed a combined diagnostic analysis of the significant acylcarnitines to evaluate their combined potential in distinguishing between the groups. The results demonstrated strong discriminative power, with an AUC of 0.933 between TBM and NMC, 0.855 between TBM and VM, and moderate discrimination between VM and NMC (0.709). (Figs. 4M–O).

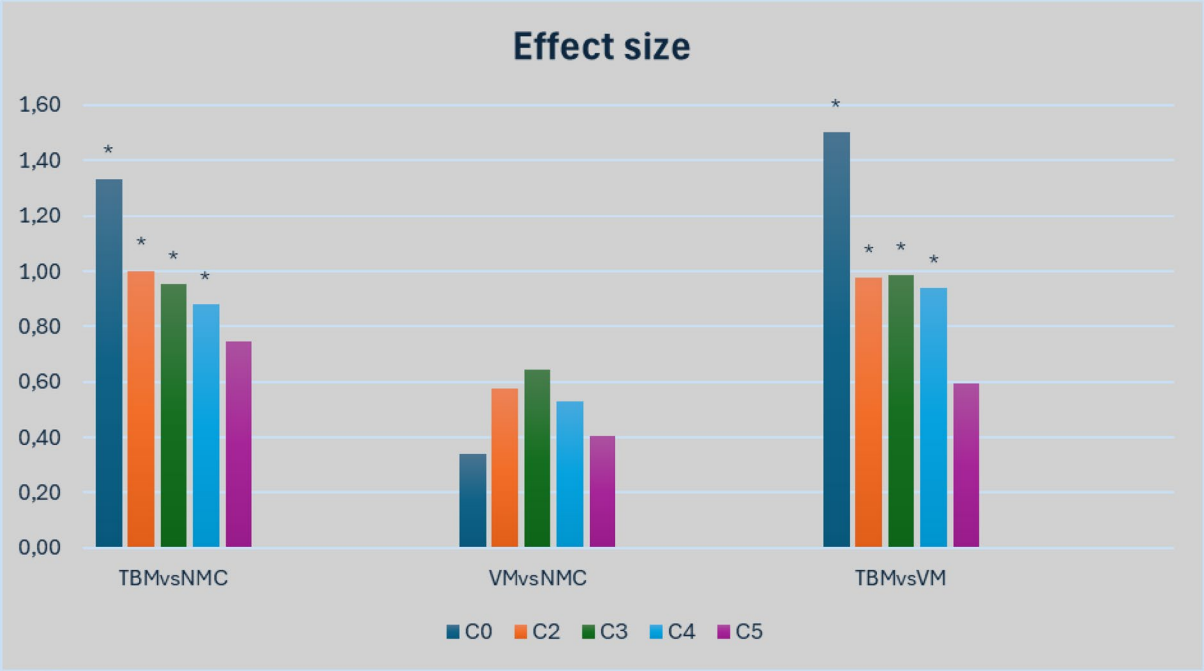

Fig. 3. Cohen's d-values of significant metabolites ($p < 0.05$). Metabolites with a Cohen's d-value > 0.8 were considered to have a large effect and were included for further statistical analysis. Cohen's d-value > 0.8 is indicated by (*).

Correlation with clinical, CSF, and MRI findings

Correlation analysis was conducted between the significant acylcarnitines and clinical characteristics, CSF features, and MRI parameters (Table 1). None of the acylcarnitines demonstrated a significant correlation with clinical characteristics ($r < 0.5$, $p > 0.05$) (Fig. S4). Instead, L-carnitine, acetylcarnitine and propionylcarnitine showed a strong positive correlation ($r > 0.5$, $p < 0.05$, Fig. 5A). Figure 5B shows a correlation analysis of CSF features, which revealed a significant positive correlation between acetylcarnitine and both leukocytes and lymphocytes in CSF ($r > 0.5$, $p < 0.05$). This positive correlation was also observed between propionylcarnitine and lymphocytes ($r > 0.5$, $p < 0.05$). In contrast, L-carnitine showed a significant but weak correlation with CSF features ($r < 0.5$, $p < 0.05$), while butyrylcarnitine demonstrated no significant correlation with CSF features. Correlation with MRI revealed a significantly strong positive relationship between L-carnitine and basal enhancement and hydrocephalus. Acetylcarnitine and propionylcarnitine demonstrated a positive correlation with only hydrocephalus. In contrast, butyrylcarnitine showed no significant correlation with MRI findings (Fig. 5C).

Discussion

In this study, we used LC-MS/MS targeted acylcarnitine analysis to characterise the CSF acylcarnitine profile of paediatric TBM and offer a comparison to NMC and VM. We correlated significant metabolites with CSF features and neuroimaging findings. We identified five significantly elevated levels of acylcarnitines (free carnitine (C0); acetylcarnitine (C2); propionylcarnitine (C3); butyrylcarnitine (C4); isovalerylcarnitine (iC5)) in TBM compared to control and VM. Short-chain acylcarnitines demonstrated the most pronounced alterations, while medium- and long-chain acylcarnitines (decanoylcarnitine (C10); dodecanoylcarnitine (C12); tetradecanoylcarnitine (C14) showed no significant differences across the groups.

Acylcarnitines are a diverse class of metabolites that play a crucial role in mitochondrial β-oxidation, a process essential for energy production. Owing to the structural diversity of their acyl groups, acylcarnitines are commonly categorised based on carbon chain length (short-, medium-, long-, and very long-chain acylcarnitines, as well as by the presence of structural modifications, such as hydroxyl or carboxyl groups, and the existence of isomeric or isobaric forms. Previous studies have highlighted the complexity of the acylcarnitine metabolome. For instance, Giesbertz et al.[36] quantified 56 distinct acylcarnitine species in plasma and tissue samples using LC-MS/MS. Yu et al.[37] proposed a comprehensive LC-HRMS strategy that enabled the identification of over 700 acylcarnitine species. Furthermore, Dambrova et al.[38] described the nomenclature and metabolic origin of over 1200 acylcarnitines. A list of acylcarnitines, including potential isomers and isobars, is provided in Table S2; however, it should be noted that the full acylcarnitine spectrum may extend beyond those listed.

Acylcarnitines can exist as isomers with identical molecular weights, making their distinction challenging. In our study, we relied heavily on isotope-labelled internal standards, a panel of known acylcarnitine standards, including known isomeric forms, and a carefully optimized chromatographic method to achieve separation and accurate compound identification. Individual analyte peaks showed co-elution with their corresponding

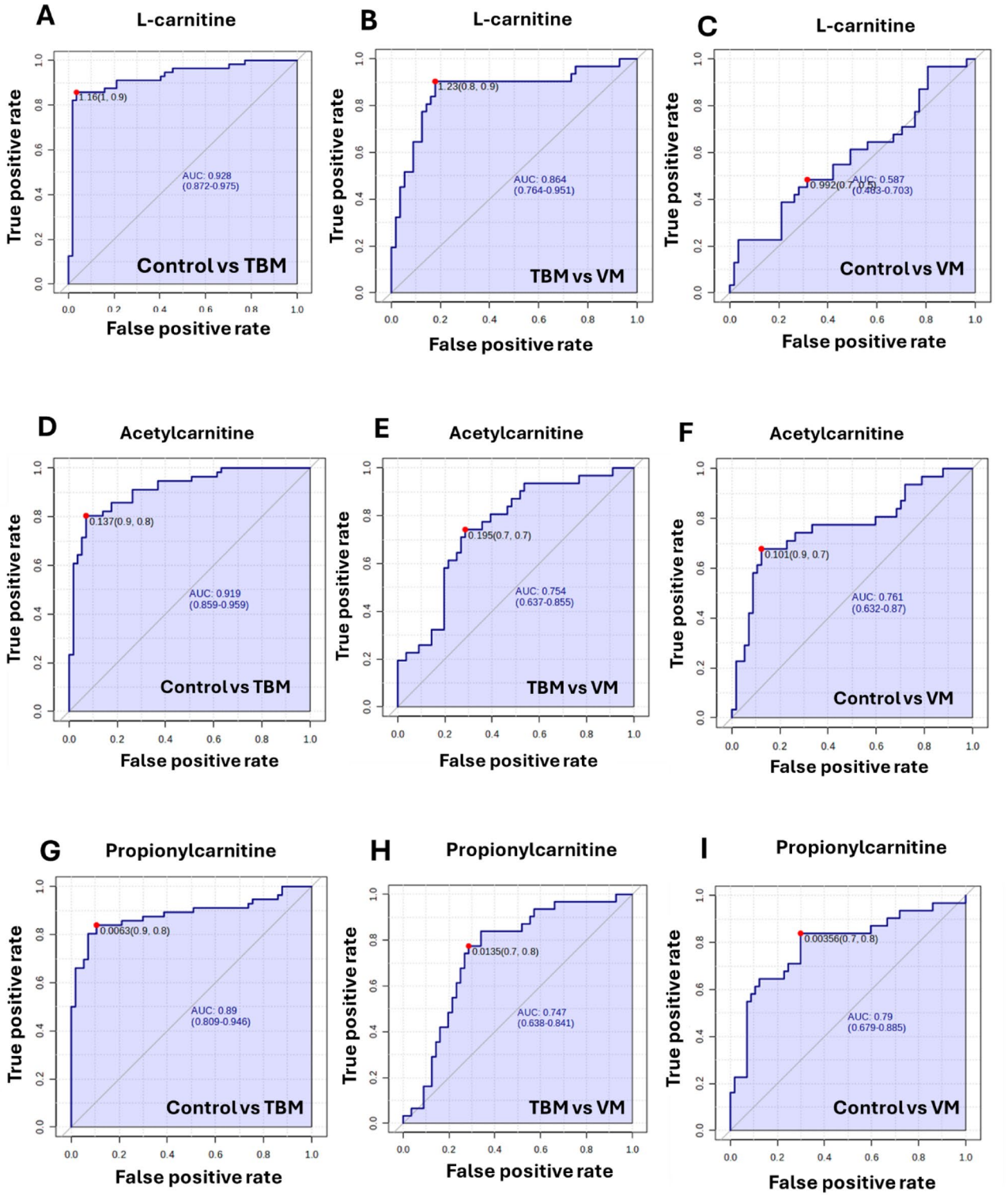

Fig. 4. Receiver operating characteristics (ROC) curves of potential markers of TBM. **A-C**: L-carnitine; **D-F**: acetylcarnitine; **G-I**: propionylcarnitine; **J-L**: butyrylcarnitine; **M-O**: combination of L-carnitine, acetylcarnitine, propionylcarnitine, and butyrylcarnitine.

internal standards, as demonstrated in Figures S2–S5. While we are confident in the accuracy of our compound identification, we acknowledge that the presence of co-eluting or undetected isomers remains a possibility, which may be a limitation of the study.

Free carnitine emerged as a promising diagnostic marker, specifically distinguishing TBM from both NMC and VM, but not between NMC and VM, highlighting its potential specificity for TBM. Furthermore,

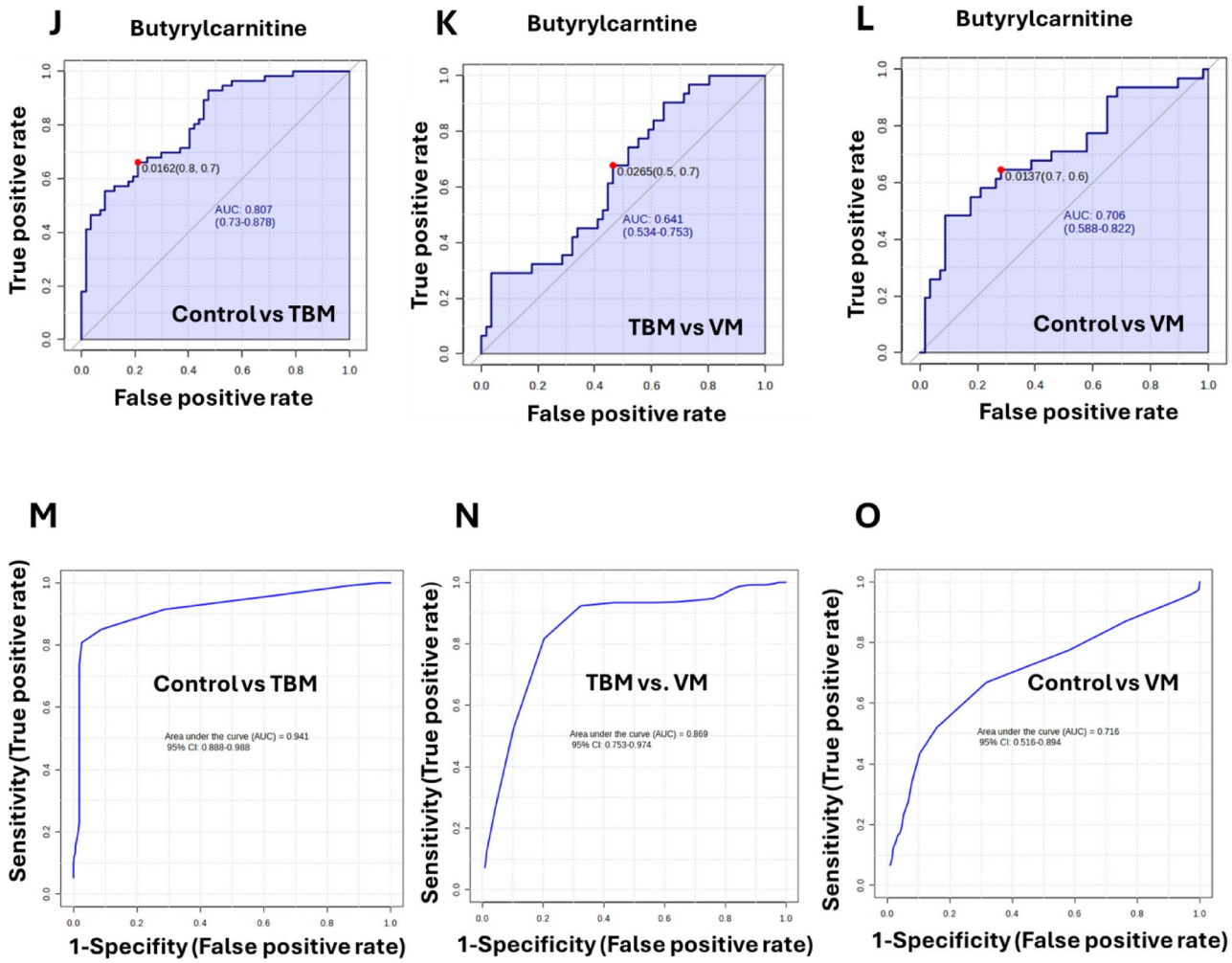

Fig. 4. (continued)

free carnitine correlated positively with hydrocephalus and basal enhancement, hallmark symptoms of TBM. Basal enhancement reflects an intense inflammation at the base of the brain, and hydrocephalus results from impaired CSF drainage due to this intense inflammation[39]. This relationship indicates that free carnitine could be influenced by, or serve as a marker for, the severity of neuroinflammation and associated structural brain changes in TBM. Its correlation with these critical symptoms further supports its potential role as a specific marker for TBM diagnosis and severity. Interestingly, free carnitine showed no significant association with CSF cell count, while acetylcarnitine and propionylcarnitine demonstrated a strong positive correlation with leukocytes, particularly lymphocytes. However, despite this positive correlation, they are not strong predictors for distinguishing between TBM and VM, likely due to similar or slightly different cell counts. In our cohort, the PCR test for enterovirus was positive in 42% of samples from patients with definite viral meningitis. This finding may explain the elevated leukocyte counts, particularly the increase in lymphocytes, as enteroviral meningitis is known to present with a predominance of lymphocytes and possible PMN predominance in the early stages[40]. Butyrylcarnitine showed no relationship with clinical data, CSF features, or neuroimaging findings despite its significant and strong role in differentiating between the groups.

AI-Mehlafi et al.[28] reported elevated levels of butyrylcarnitine and isovalerylcarnitine in the CSF of Herpes simplex virus (HSV), declaring these metabolites as the key contributors to biomarkers for viral CNS infections. These alterations were attributed to mitochondrial dysfunction. The study further reported that free carnitine and propionylcarnitine contributed to differentiating viral CNS infections from autoimmune neuroinflammation and controls. However, they were not identified as the best biomarkers for viral CNS infections. In contrast, our study uniquely compared the acylcarnitine profile of TBM and VM and identified short-chain acylcarnitines (free carnitine, acetylcarnitine and propionylcarnitine) as some of the most significant markers for TBM, suggesting that the alteration in these metabolites may reflect metabolic dysregulation specific to mycobacterial infection. However, collectively, these studies underscore the need for further investigation into carnitine metabolism across a broader spectrum of bacterial and viral neuroinfectious diseases.

A study on neurosyphilis, a bacterial neuroinfection, reported increased levels of butyrylcarnitine and palmitoylcarnitine in CSF, which were associated with increased risk of cardiovascular diseases[29]. As our

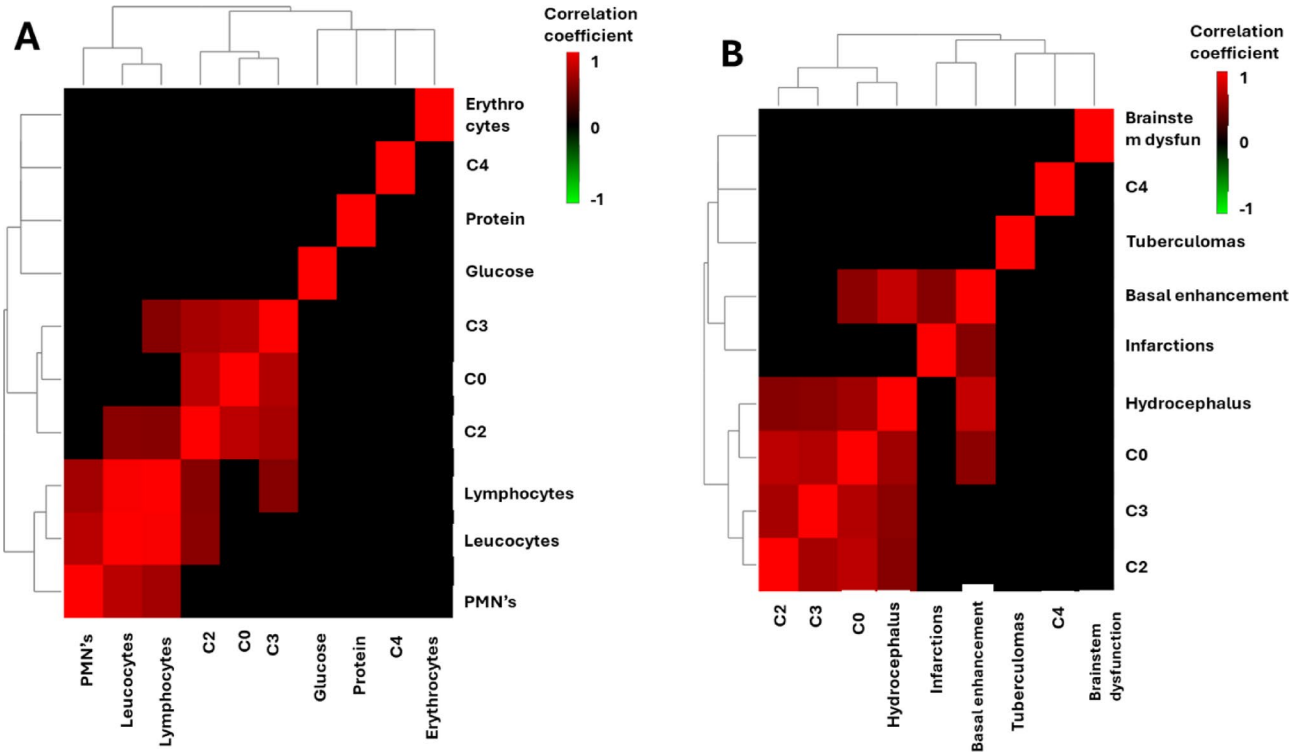

Fig. 5. Correlations of significant acylcarnitines with (**A**) CSF features and (**B**) neuroimaging findings. Only correlations with an r-value greater than 0.5 and a p-value less than 0.05 are shown. C0 = L-carnitine; C2 = acetylcarnitine; C3 = propionylcarnitine; C4 = butyrylcarnitine.

findings show, butyrylcarnitine was also elevated in TBM, although it did not correlate with CSF or MRI findings. However, it effectively distinguished between groups, especially between NMC and TBM, suggesting that butyrylcarnitine may reflect broader metabolic disturbances in bacterial infections rather than being directly linked to the specific pathophysiology of TBM.

Alteration in free carnitine seems to be directly linked to TBM or bacterial infections. Tomalka et al.[22] reported an increased elevation of multiple carnitines and lactate in the CSF of adults with TBM. A previous NMR study[23] also identified free carnitine as a distinct metabolite differentiating paediatric TBM from controls. Carnitine is widely recognized for its crucial role in β-oxidation, as it transports long-chain fatty acids into the mitochondria[41]. Dysregulation of carnitines may reflect impairment of mitochondrial β-oxidation of fatty acids. B-oxidation of fatty acids typically occurs when the body experiences a high energy demand. In TBM, energy demand is elevated due to the metabolic requirements of *M.tb*, neuroinflammation, and immune responses, as supported by various studies showing reduced CSF glucose and increased CSF lactate alongside disrupted energy metabolism pathways. Increased lactate suggests increased glycolysis, a key marker of enhanced energy production[19,20,23,42–44]. In this context, altered free carnitine in TBM may imply that the body is mobilising carnitine to support the β-oxidation of fatty acids. However, the accumulation of short-chain acylcarnitines may result from incomplete β-oxidation, likely due to mitochondrial dysfunction, leading to their release into the extracellular space[28]. The lack of alteration in long-chain acylcarnitines may indicate insufficient mobilisation into the mitochondria, thereby contributing to elevated free carnitine levels.

Another potential explanation for the altered short-chain acylcarnitines in TBM is a shift in lipid metabolism. During prolonged energy demand, cells may preferentially metabolise ketone bodies rather than fatty acids, primarily because the transport of fatty acids across the BBB is limited[45]. In such cases, ketone bodies serve as the optimal energy source. While evidence from animal studies indicates that astrocytes and neurons can utilise ketone bodies[46,47], there is limited information on the specific human brain cell type involved in ketone metabolism. The study of Dai et al.[27] reported increased synthesis and degradation of ketone bodies and increased levels of unsaturated fatty acids in TBM, suggesting a possible shift toward ketone metabolism as an alternative energy source. Additionally, lipid turnover in the brain could produce short-chain acylcarnitines as byproducts, contributing to their extracellular accumulation. It is also important to note that carnitines play roles beyond fatty acid transport into the mitochondria. For example, brain acylcarnitines are involved in lipid synthesis[25], and their alteration could also reflect disruptions in lipid metabolism. Future targeted lipidomics studies could provide insights into the relationship between lipids and carnitines, offering valuable information on the pathophysiology of TBM. The limitations of our study include the fact that all samples were collected from a single centre, which restricted our ability to perform external validation. Additionally, our control group was not composed entirely of healthy individuals. At the same time, they were confirmed not to have meningitis; instead, they presented with other clinical symptoms, such as fever related to a bacterial or viral infection. Lastly, further

studies involving other forms of meningitis, such as bacterial meningitis, are needed to confirm the specificity of free carnitine to TBM. If free carnitine is found to be specific to TBM, this would support its potential as an early diagnostic marker. In high TBM prevalence settings, especially among paediatric patients, this could significantly improve clinical outcomes by enabling earlier diagnosis and timely initiation of treatment.

Conclusion

Free carnitine showed strong potential as a biomarker for TBM. Its inability to differentiate VM from NMC further underscores its specificity to TBM rather than just being a general marker of CNS immune response. Furthermore, free carnitine strongly correlates with basal enhancement and hydrocephalus, key neuroradiological markers of TBM. These findings not only provide insights into the metabolic underpinnings of TBM but also offer a clinically valuable diagnosis and intervention that could potentially improve patient outcomes. Based on our findings, future TBM studies should also consider CSF lipidomics to improve our understanding of carnitine mechanisms in TBM.

Data availability

Data will be made available by request with the corresponding author.

Received: 7 March 2025; Accepted: 5 August 2025
Published online: 11 August 2025

References

1. Zaharie, S-D. et al. The immunological architecture of granulomatous inflammation in central nervous system tuberculosis. *Tuberculosis* **125**, 102016 (2020).
2. Gutiérrez-González, L. H. et al. Immunological aspects of diagnosis and management of childhood tuberculosis. *Infect. Drug Resist.* **14**, 929–946 (2021).
3. World Health Organisation (WHO). WHO global report. 2019. Report No.: WHO/CDS/TB/2019.15 | ISBN: 978-92-4-156571-4. (2019).
4. du Preez, K. et al. Global burden of tuberculous meningitis in children aged 0–14 years in 2019: A mathematical modelling study. *Lancet Global Health.* **13** (1), e59–e68 (2025).
5. World Health Organization (WHO). *Global Tuberculosis Report 2024* (World Health Organization, 2024).
6. Basu Roy, R. et al. Defeating paediatric tuberculous meningitis: Applying the WHO defeating meningitis by 2030: Global roadmap. *Microorganisms* **9** (4), 857 (2021).
7. du Preez, K. et al. Tuberculous meningitis in children: A forgotten public health emergency. *Front. Neurol.* **13**, 751133 (2022).
8. Marais, S. et al. Tuberculous meningitis: A uniform case definition for use in clinical research. *Lancet. Infect. Dis.* **10** (11), 803–812 (2010).
9. Van Well, G. T. et al. Twenty years of pediatric tuberculous meningitis: A retrospective cohort study in the Western cape of South Africa. *Pediatrics* **123** (1), e1–e8 (2009).
10. Chiang, S. S. et al. Treatment outcomes of childhood tuberculous meningitis: A systematic review and meta-analysis. *Lancet. Infect. Dis.* **14** (10), 947–957 (2014).
11. Madan, M., Sehgal, R., Tuli, I. P., Mehta, A. & Gera, R. Outcome of tuberculous meningitis in children aged 9 months to 12 years at the end of intensive phase of treatment. *Indian J. Tuberculosis.* **70**, S104–S15 (2023).
12. Stadelman, A. M. et al. Cerebrospinal fluid AFB smear in adults with tuberculous meningitis: A systematic review and diagnostic test accuracy meta-analysis. *Tuberculosis* **135**, 102230 (2022).
13. Bahr, N. C. et al. Diagnostic accuracy of Xpert MTB/RIF ultra for tuberculous meningitis in HIV-infected adults: A prospective cohort study. *Lancet. Infect. Dis.* **18** (1), 68–75 (2018).
14. Cresswell, F. V. et al. Xpert MTB/RIF ultra for the diagnosis of HIV-associated tuberculous meningitis: A prospective validation study. *Lancet. Infect. Dis.* **20** (3), 308–317 (2020).
15. Donovan, J. et al. Xpert MTB/RIF ultra versus Xpert MTB/RIF for the diagnosis of tuberculous meningitis: A prospective, randomised, diagnostic accuracy study. *Lancet. Infect. Dis.* **20** (3), 299–307 (2020).
16. Manyelo, C. M. et al. Validation of host cerebrospinal fluid protein biomarkers for early diagnosis of tuberculous meningitis in children: A replication and new biosignature discovery study. *Biomarkers* **27** (6), 549–561 (2022).
17. Visser, D. H. et al. Host immune response to tuberculous meningitis. *Clin. Infect. Dis.* **60** (2), 177–187 (2015).
18. Zhang, P. et al. Mass spectrometry-based metabolomics for tuberculosis meningitis. *Clin. Chim. Acta.* **483**, 57–63 (2018).
19. Mason, S. & Solomons, R. CSF metabolomics of tuberculous meningitis: A review. *Metabolites* **11** (10), 661 (2021).
20. Mason, S., Reinecke, C. J., Solomons, R. & Van Furth, A. Tuberculous meningitis in infants and children: Insights from nuclear magnetic resonance metabolomics. *S. Afr. J. Sci.* **112** (3–4), 1–8 (2016).
21. Samuel, V., Solomons, R. & Mason, S. Targeted metabolomics investigation of metabolic markers of Mycobacterium tuberculosis in the cerebrospinal fluid of paediatric patients with tuberculous meningitis. *PLoS ONE.* **19** (12), e0314854 (2024).
22. Tomalka, J. et al. Combined cerebrospinal fluid metabolomic and cytokine profiling in tuberculosis meningitis reveals robust and prolonged changes in immunometabolic networks. *Tuberculosis* **144**, 102462 (2024).
23. Van Zyl, C. D. W., Loots, D. T., Solomons, R., Van Reenen, M. & Mason, S. Metabolic characterization of tuberculous meningitis in a South African paediatric population using 1H NMR metabolomics. *J. Infect.* **81** (5), 743–752 (2020).
24. Zhang, P. et al. 1H nuclear magnetic resonance-based metabolic profiling of cerebrospinal fluid to identify metabolic features and markers for tuberculosis meningitis. *Infect. Genet. Evol.* **68**, 253–264 (2019).
25. Jones, L. L., McDonald, D. A. & Borum, P. R. Acylcarnitines: Role in brain. *Prog. Lipid Res.* **49** (1), 61–75 (2010).
26. Plaatjie, O. N., van Furth, A. M. T., Van Der Kuip, M. & Mason, S. LC–MS metabolomics and lipidomics in cerebrospinal fluid from viral and bacterial CNS infections: A review. *Front. Neurol.* **15**, 1403312 (2024).
27. Dai, Y-N. et al. Identification of potential metabolic biomarkers of cerebrospinal fluids that differentiate tuberculous meningitis from other types of meningitis by a metabolomics study. *Oncotarget* **8** (59), 100095 (2017).
28. Al-Mekhlafi, A. et al. Elevated phospholipids and acylcarnitines C4 and C5 in cerebrospinal fluid distinguish viral CNS infections from autoimmune neuroinflammation. *J. Transl. Med.* **21** (1), 776 (2023).
29. Qi, S. et al. Novel biochemical insights in the cerebrospinal fluid of patients with neurosyphilis based on a metabonomics study. *J. Mol. Neurosci.* **69**, 39–48 (2019).
30. Donald, P. et al. Pediatric meningitis in the Western cape Province of South Africa. *J. Trop. Pediatr.* **42** (5), 256–261 (1996).
31. Terburgh, K., Coetzer, J., Lindeque, J. Z., van der Westhuizen, F. H. & Louw, R. Aberrant BCAA and glutamate metabolism linked to regional neurodegeneration in a mouse model of Leigh syndrome. *Biochim. Et Biophys. Acta (BBA)-Mol. Basis Disease.* **1867** (5), 166082 (2021).

32. Van Toorn, R., Springer, P., Laubscher, J. & Schoeman, J. Value of different staging systems for predicting neurological outcome in childhood tuberculous meningitis. *Int. J. Tuberc. Lung Dis.* **16** (5), 628–632 (2012).
33. Jerrard, D. A., Hanna, J. R. & Schindelheim, G. L. Cerebrospinal fluid. *J. Emerg. Med.* **21** (2), 171–178 (2001).
34. Tan, Q. C. et al. Correlation between blood glucose and cerebrospinal fluid glucose levels in patients with differences in glucose metabolism. *Front. Neurol.* **14**, 1103026 (2023).
35. Hosmer, D. & Lemeshow, S. Applied logistic regression. 2nd ed (Wiley, 2000).
36. Giesbertz, P., Ecker, J., Haag, A., Spanier, B. & Daniel, H. An LC-MS/MS method to quantify acylcarnitine species including isomeric and odd-numbered forms in plasma and tissues. *J. Lipid Res.* **56** (10), 2029–2039 (2015).
37. Yu, D. et al. Strategy for comprehensive identification of acylcarnitines based on liquid chromatography–high-resolution mass spectrometry. *Anal. Chem.* **90** (9), 5712–5718 (2018).
38. Dambrova, M. et al. Acylcarnitines: Nomenclature, biomarkers, therapeutic potential, drug targets, and clinical trials. *Pharmacol. Rev.* **74** (3), 506–551 (2022).
39. Ma, Q. et al. MRI-based radiomics signature for identification of invisible basal cisterns changes in tuberculous meningitis: A preliminary multicenter study. *Eur. Radiol.* **32** (12), 8659–8669 (2022).
40. Shahan, B., Choi, E. Y. & Nieves, G. Cerebrospinal fluid analysis. *Am. Fam. Phys.* **103** (7), 422–428 (2021).
41. Adeva-Andany, M. M., Carneiro-Freire, N., Seco-Filgueira, M., Fernández-Fernández, C. & Mouriño-Bayolo, D. Mitochondrial β-oxidation of saturated fatty acids in humans. *Mitochondrion* **46**, 73–90 (2019).
42. Liu, C. et al. High cerebrospinal fluid lactate concentration at 48 h of hospital admission predicts poor outcomes in patients with tuberculous meningitis: A multicenter retrospective cohort study. *Front. Neurol.* **13**, 989832 (2022).
43. Solomons, R. et al. The diagnostic value of cerebrospinal fluid chemistry results in childhood tuberculous meningitis. *Child's Nerv. Syst.* **31**, 1335–1340 (2015).
44. Zou, Y., He, J., Guo, L., Bu, H. & Liu, Y. Prediction of cerebrospinal fluid parameters for tuberculous meningitis. *Diagn. Cytopathol.* **43** (9), 701–704 (2015).
45. Morris, A. Cerebral ketone body metabolism. *J. Inherit. Metab. Dis.* **28** (2), 109–121 (2005).
46. Tildon, J. T., McKenna, M. C. & Stevenson, J. H. Transport of 3-hydroxybutyrate by cultured rat brain astrocytes. *Neurochem. Res.* **19**, 1237–1242 (1994).
47. Tildon, J. T. & Roeder, L. M. Transport of 3-hydroxy [3-14 C] butyrate by dissociated cells from rat brain. *Am. J. Physiol.-Cell Physiol.* **255** (2), C133–C9 (1988).

Acknowledgements

We thank Brenda Klopper for providing acylcarnitine isotopes and for her invaluable assistance with method optimisation. We also thank Carien Van der Berg and Tarien Jacobs for their continuous guidance and training on the LC-MS/MS instrument. We also thank Talulani Marangeni and Renzo Snyders for assisting with sample preparation training.

Author contributions

Conceptualization: Shayne Mason; Data curation: Ontefetse Neo Plaatjie and Regan Solomons; Formal analysis: Ontefetse Neo Plaatjie; Funding acquisition: Martijn van der Kuip and A. Marceline Tutu van Furth; Investigation: Ontefetse Neo Plaatjie; Methodology: Ontefetse Neo Plaatjie and Shayne Mason; Project administration: Martijn van der Kuip and A. Marceline Tutu van Furth; Resources: Regan Solomons; Supervision: Shayne Mason, Martijn van der Kuip and A. Marceline Tutu van Furth; Writing – original draft: Ontefetse Neo Plaatjie; Writing – review & editing: Regan Solomons, Martijn van der Kuip, A. Marceline Tutu van Furth, and Shayne Mason.

Funding

Mr. Willem Backhuys Roozeboomstichting in the Netherlands.

Competing interests

The authors declare no competing interests.

Additional information

Supplementary Information The online version contains supplementary material available at https://doi.org/10.1038/s41598-025-15000-0.

Correspondence and requests for materials should be addressed to S.M.